Published in final edited form as:
Dev Biol. 2008 August 1; 320(1): 278–288. doi:10.1016/j.ydbio.2008.05.541.

Ribbon Modulates Apical Membrane during Tube Elongation through Crumbs and Moesin

Bilal E. Kerman[1,*], **Alan M. Cheshire**[1,2,*], **Monn Monn Myat**[3], and **Deborah J. Andrew**[1,†]

1*Department of Cell Biology, Johns Hopkins University School of Medicine, Baltimore, MD 21205, USA*

2*Department of Biomedical Engineering, Johns Hopkins University School of Medicine, Baltimore, MD 21205, USA*

3*Department of Cell and Developmental Biology, Weill Medical College, Cornell University, New York, NY 10021, USA*

Abstract

Although the formation and maintenance of epithelial tubes is essential for the viability of multi-cellular organisms, our understanding of the molecular and cellular events coordinating tubulogenesis is relatively limited. Here, we focus on the activities of Ribbon, a novel BTB-domain containing nuclear protein, in the elongation of two epithelial tubes: the Drosophila salivary gland and trachea. We show that Ribbon interacts with Lola Like, another BTB-domain containing protein required for robust nuclear localization of Ribbon, to upregulate *crumbs* expression and downregulate Moesin activity. Our ultrastructural analysis of *ribbon* null salivary glands by TEM reveals a diminished pool of subapical vesicles and an increase in microvillar structure, cellular changes consistent with the known role of Crumbs in apical membrane generation and of Moesin in the cross-linking of the apical membrane to the subapical cytoskeleton. Furthermore, the subapical localization of Rab11, a small GTPase associated with apical membrane delivery and rearrangement, is significantly diminished in *ribbon* mutant salivary glands and tracheae. These findings suggest that Ribbon and Lola Like function as a novel transcriptional cassette coordinating molecular changes at the apical membrane of epithelial cells to facilitate tube elongation.

Keywords

Apical membrane; Crumbs; Lola Like; Moesin; Rab11; Ribbon; tube morphogenesis

Introduction

Tubular organs are essential for life in all multicellular organisms, including humans. Examples of tubular organs include the lungs and vasculature, which provide for gas and nutrient exchange, the kidneys, which maintain homeostatic fluid balance, the exocrine pancreas, which secretes enzymes for digestion, and the endocrine pancreas, which secretes hormones that regulate blood glucose levels and growth. Organs such as the salivary glands and lacrimal glands, which provide lubrication and secrete anti-microbial peptides, are also organized into

†Contact: dandrew@jhmi.edu; phone: 410−614−2722; fax: 410−955−4129.
*These authors contributed equally to this work.

tubular epithelial structures. Not surprisingly, defects in tube formation and/or maintenance from birth defects such as spina bifida to vascular diseases such as atherosclerosis and arterial thrombosis account for a huge proportion of the health care problems in developed nations. Despite the importance of tube formation and maintenance in human development and disease, our understanding of how tubular organ size and shape is established is quite limited, although recent studies in model organisms suggest key roles for regulated apical secretion and modifications of apical secretions in both diametrical tube expansion and tube length control (Seshaiah et al., 2001; Tsarouhas et al., 2007).

The Drosophila salivary gland (SG), which comprises two simple unbranched tubes specialized for secretion, and trachea (TR), a highly branched tubular network specialized for oxygen delivery, have become useful models for elucidating the molecular and cellular mechanisms of epithelial tube morphogenesis (Kerman et al., 2006). The SG forms from two placodes of polarized epithelial cells found in an anterior region of the embryo. Through regulated, sequential cell shape changes, the cells internalize to form paired tubular organs that elongate and migrate along several tissues to attain their final correct position in the embryo (Bradley et al., 2003; Myat and Andrew, 2000a; Myat and Andrew, 2000b; Vining et al., 2005). The trachea arises from 20 smaller placodes, ten on each side, of polarized epithelial cells. The tracheal primordia invaginate through a combination of cell shape changes and rearrangement to form internalized tracheal sacs (Nishimura et al., 2007). Subsets of cells within each sac then migrate in stereotypical directions to form branched structures that ultimately fuse to form a contiguous tubular network that carries oxygen from two posterior openings to all of the cells in the animal (Manning and Krasnow, 1993). Several transcription factors and their transcriptional targets have been implicated in either SG or TR morphogenesis. Fork head and Huckebein are transcription factors required for early stages of SG invagination and tube elongation, respectively, whereas the transcription factor Trachealess and its downstream target Breathless, an FGF receptor, are critical for tracheal invagination and subsequent branch migration, respectively (Isaac and Andrew, 1996; Klämbt et al., 1992; Myat and Andrew, 2000a; Myat and Andrew, 2000b; Weigel et al., 1989; Wilk et al., 1996; Zelzer and Shilo, 2000).

ribbon (*rib*) is required for the morphogenesis of many embryonic tissues including both the SG and TR (Bradley and Andrew, 2001; Jack and Myette, 1997; Shim et al., 2001). In *rib* mutants, the SG forms a tube that fails to elongate, and the TR exhibits delayed migration, ultimately failing to form a subset of branches, most notably the dorsal trunk (DT), which is the major artery connecting the trachea along the anterior-posterior body axis (Bradley and Andrew, 2001; Shim et al., 2001). *rib* encodes a 661-residue protein of the poorly understood Broad Tramtrack Bric-a-brac (BTB) domain transcription factor family that is composed of a BTB domain, a Pipsqueak DNA-binding domain, nuclear localization sequences, putative MAPK phosphorylation sites, and a coiled-coil motif (Bradley and Andrew, 2001; Shim et al., 2001). The molecular basis for the *rib* mutant phenotype is unknown, but rescue experiments have shown that Rib functions in a tissue-autonomous manner (Bradley and Andrew, 2001).

The identification of interacting molecules as well as downstream target genes is key to understanding how Rib mediates tube elongation. Indeed, at least two transcriptional targets of Rib have been identified through genome-wide screens: *serpentine* (*serp*) and *vermiform* (*verm*) (Luschnig et al., 2006). These neighboring genes, whose full level of expression in late embryonic stages requires *rib*, encode proteins that are secreted into the lumen and contain chitin binding and deacetylation domains. Interestingly, the loss of these genes does not give rise to Rib-like TR defects; instead their loss results in excessively long tracheal tubes (Luschnig et al., 2006; Wang et al., 2006), a defect opposite to that observed in the TR and SG of *rib* mutants. Thus, the identification of *serp* and *verm* as Rib target genes is likely revealing later roles for Rib in limiting tube size. Here, we focus on the earlier role of Rib in tube

elongation in the SG and TR dorsal trunk. We identify and characterize the role of a Rib interacting protein known as Lola like (Lolal) in the SG and TR and we identify key downstream molecular targets that mediate tube elongation.

Materials and methods

Fly strains and genetics

Flies were grown and kept on standard cornmeal/agar medium. The fly lines used are given in Table 1. The UAS-Gal4 expression system (Brand and Perrimon, 1993) was used for tissue-specific expression. p-values were calculated using an online chi-square test calculator (Preacher, 2001).

Immunohistochemistry and in situ hybrization

Embryo fixation and staining were performed as described previously (Reuter et al., 1990). Antibodies used are given in Table 2. Whole-mount in situ hybridizations were performed as described previously (Lehmann and Tautz, 1994). Embryos were visualized by Nomarski optics using a Zeiss Axiophot microscope or by fluorescence using a Zeiss LSM510 microscope. For protein level comparisons, images were taken under identical optical and electronic conditions. Pixel intensities were analyzed using Zeiss image acquisition software and calculations were performed in Excel (Microsoft).

Real-time PCR

Homozygous embryos were selected by lack of GFP expression through an automated embryo sorter (Union Biometrica), confirmed visually on a dissecting microscope, and frozen in liquid nitrogen. mRNA was isolated using a Micro-FastTrack 2.0 kit (Invitrogen). *crumbs* (*crb)* mRNA levels were analyzed quantitatively by real-time PCR performed in triplicate using SuperScript II reverse transcriptase (Invitrogen), iQ SYBR Green Supermix (Biorad), and the iQ5 real-time PCR detection system (Biorad), and calculations were performed using the Pfaffl Method (Pfaffl, 2001). Gene-specific primer sequences used for quantification of *crb* transcript were: 5’-GATCGCGCGGCAAGCATATT-3’ (forward) and 5’-GGTCCATCCAGAAGGCAACC-3’ (reverse). Reference control was *eIF-4a* transcript, amplified using the primer pair: 5’-TCGGTAATCTTCTGCAACACCCGT-3’ (forward) and 5’-CATCAATACCGCGCGCCAGTAAAT-3’ (reverse).

Transmission electron microscopy

Wild -type (WT) and homozygous *rib* embryos were selected, processed for TEM and analyzed on a Philips EM120 as previously described (Myat and Andrew, 2000a). Thin sections were acquired throughout the lumena of three WT and three *rib* stage 12 SGs, and sections were analyzed at magnifications from 980x to 15000x.

Results

Lola Like serves as a novel partner for Rib in SG and TR morphogenesis

To choose the best *rib* allelic combination and to resolve discrepancies regarding the reported *rib* mutant defects, we evaluated the severity of SG and TR defects in the alleles rib^{P7} and rib^{1}, which encode premature stops at residues 22 and 283, respectively, and in the deficiency $Df(2R)rib^{ex12}$, which removes *rib* and at least 25 other genes (Bradley and Andrew, 2001; Shim et al., 2001). Whereas wild-type (WT) stage 12 SGs turned and migrated at a high frequency, SGs of all *rib* alleles frequently failed to turn and migrate (Figs. 1A-E). In addition, whereas the WT stage 14 TR dorsal trunk (DT) extended and fused at a high frequency, DTs of all *rib* alleles exhibited only partial extension at this stage (Figs. 1H-L). Both rib^{P7} and

rib^{1} TR extended relatively normal dorsal (Figs. 1H-L) and visceral (data not shown) branches as reported by Bradley and Andrew (2001), indicating that *rib* is not absolutely required for primary branch formation as proposed by Shim et al. (2001). Additionally, whereas the SG defects showed the expected allelic series of *Df(2R)rib*^{ex12} > *rib*^{P7} > *rib*^{1}/*rib*^{P7} > *rib*^{1}, the TR defects exhibited the surprising allelic series of *Df(2R)rib*^{ex12} > *rib*^{1}/*rib*^{P7} > *rib*^{1} > *rib*^{P7}, suggesting the presence of a recessive TR-specific modifier on the *rib*^{P7} chromosome. We thus chose the transallelic combination *rib*^{1}/*rib*^{P7} for further analysis of SG and TR morphogenic defects and, unless otherwise noted, performed all subsequent experiments with this genotype.

Rib localizes to the nucleus and is thought to function as a transcription factor. Lolal, which is expressed ubiquitously in the embryo and is another nuclearly-localized member of the BTB transcription factor family, was recently identified as a binding partner for Rib in a genome-wide yeast two-hybrid screen (Faucheux et al., 2003; Giot et al., 2003; Siegmund and Lehmann, 2002). In support of this interaction, maternal and zygotic mutants of the hypomorphic *lolal* allele *lolal*^{K02512} (*lolal*^{K02512,mz}) exhibited *rib*-like SG and DT phenotypes (Figs. 1F, M), and the removal of one copy of *rib* in *lolal*^{K02512,mz} mutants significantly increased the frequency of defects in the SG (from 44.0% to 59.2%, p=0.016; Fig. 1G) but did not significantly increase defects in the DT (from 44.7% to 50.0%, p=0.689; Fig. 1N). In addition, previous studies have shown that Rib fails to localize to nuclei in the *rib*^{2} allele (P.L. Bradley and D.J. Andrew, unpublished), which encodes a mutation of a highly conserved BTB domain residue that could mediate binding to Lolal (Bradley and Andrew, 2001; Shim et al., 2001). Indeed, whereas Rib localized robustly to nuclei of WT SG, TR, and adjacent mesoderm (Figs. 1O, R), it failed to localize to nuclei in these tissues in *rib*^{2} mutants (Figs. 1P, S). Interestingly, Rib exhibited only weak nuclear localization in the SG and TR of *lolal*^{K02512,mz} mutants but maintained robust nuclear localization in the adjacent mesoderm (Figs. 1Q, T). Thus, Lolal functions as a bona fide partner for Rib, functioning at least in part through enhanced Rib nuclear localization in epithelia.

Rib and Lolal are required for robust crb expression

Previous studies have demonstrated that *rib* mutant TR cells extend migratory projections in the appropriate direction but fail to move forward as a tissue, and that major guidance signaling pathways are intact (Bradley and Andrew, 2001; Shim et al., 2001). However, neither study identified the molecular basis for failed morphogenesis. In the course of our analysis, we noted that levels of the highly conserved apical membrane protein Crumbs (Crb) were consistently reduced in *rib* epithelia, whereas levels of another apical membrane protein, Stranded at Second (Sas), were comparable to WT. WT SGs exhibited high levels of both Sas and Crb during invagination and posterior migration (Figs. 2A, D). In contrast, *rib* SGs exhibited similar Sas levels but severely reduced Crb levels during these stages (Figs. 2B, E). WT TR also exhibited high levels of Sas and Crb during the formation and elongation of primary branches (Figs. 2G, J). *rib* TR, however, exhibited comparable levels of Sas but severely reduced Crb levels during these stages (Figs. 2H, K). Quantification of Crb levels by Sas-normalized pixel intensity indicated that protein levels were reduced by at least half in *rib* SG and TR (Figs. 2C, F, I, L). Thus, Crb protein levels are significantly reduced in *rib* mutants during key morphogenic stages of SG and TR development.

Since Rib is thought to function as a transcription factor, *crb* mRNA levels in *rib* and *lolal*^{K02512,mz} mutants were examined by in situ hybridization (ISH). *crb* was robustly expressed in the early WT SG and TR (Figs. 2M, Q). In contrast, *crb* expression was severely reduced in *rib* mutants (Figs. 2N, R), reduced in *lolal*^{K02512,mz} mutants (Figs. 2O, S), and slightly further reduced in *lolal*^{K02512,mz} mutants missing one copy of *rib* (Figs. 2P, T). Quantification of *crb* mRNA levels by real time-PCR indicated that total *crb* mRNA was reduced by 71% and 87% in *rib*^{1} and *rib*^{P7} embryos, respectively (Fig. 2U). Thus, Rib and

Lolal are required for robust *crb* mRNA levels in SG and TR. Since Crb has well-established roles in the regulation of apical-basal polarity and apical membrane generation (Laprise et al., 2006; Omori and Malicki, 2006; Pellikka et al., 2002; Wodarz et al., 1995) and since *rib* mutant cells do not exhibit defects in apical-basal polarity (Figs. 2-6, S1, S3-S5), we propose that *rib* mutant epithelia are deficient in regulating apical membrane dynamics during tube morphogenesis.

Rib is required for downregulation of apical Moe activity

Moesin (Moe) is another highly conserved protein that localizes predominantly to the apical surface of epithelia and has roles in apical-basal polarity and apical membrane morphology (Fievet et al., 2007; Hughes and Fehon, 2007). Moe is activated upon phosphorylation at threonine 559 and binds the FERM-binding domain of Crb and other membrane-associated proteins via its N-terminus and F-actin via its C-terminus, thus serving as an important cross-linker of apical membrane and cytoskeleton (Medina et al., 2002; Polesello et al., 2002). In contrast to the low levels of Crb protein observed in *rib* SG and TR, levels of active phosphorylated Moe (pMoe) were abnormally high in *rib* mutants. Invaginating WT and *rib* SG cells exhibited similarly high levels of apical pMoe (white arrows in Figs. 3A, B, D, E). Interestingly, after invagination, WT SG cells exhibited decreased levels of apical pMoe (yellow arrows in Figs. 3A, D) comparable to levels in the adjacent mesoderm, whereas *rib* SG cells maintained the high invagination levels of apical pMoe (yellow arrows in Figs. 3B, E). WT TR cells also exhibited mesoderm-comparable levels of apical pMoe (Figs. 3G, J), whereas *rib* TR cells exhibited notably higher levels (Figs. 3H, K), consistent with a failure to decrease apical pMoe subsequent to TR invagination. The high level of Moe activity in the SG and TR does not appear to stem from increased *moe* transcription or translation in *rib* mutants, as levels of *moe* mRNA (data not shown) and levels of total apical Moe (Fig. S2) were similar to WT. In addition, extremely high levels of pMoe were observed in a few *rib* SGs with relatively high Crb levels (data not shown), suggesting that the abnormally elevated levels of pMoe are not simply a consequence of the decreased Crb levels. Thus, *rib* is independently required for the upregulation of Crb levels and downregulation of apical Moe activity during key stages of SG and TR morphogenesis.

Though the details remain unclear, Moe is thought to be phosphorylated in response to Rho1 GTPase signaling and to play a role in feedback regulation of this signaling (Speck et al., 2003). Since *rho1* is required for SG invagination (M.M. Myat, unpublished), perturbed Rho1 activity in *rib* mutants could explain the maintenance of high apical pMoe levels. However, we found that mRNA levels for *rho1* and the downstream effectors *rho kinase* and *zipper* were unchanged in *rib* mutants, and no genetic interaction was observed between *rib* and these genes (data not shown). Another kinase known to be required for Moe phosphorylation is the Drosophila Sterile-20 kinase Slik (Hipfner et al., 2004). *slik* mRNA levels were also unchanged in *rib* mutants (data not shown). Similar to Moe, Ezrin is activated upon phosphorylation at the conserved threonine residue and, recently, Phosphatase of Regenerating Liver-3 (PRL-3) was shown to be required for dephosphorylation of this residue (Forte et al., 2008). mRNA levels of *prl-1*, the Drosophila ortholog of *prl-3*, were not significantly altered in *rib* mutants (data not shown). In light of this evidence, and since Moe appears to be activated to comparable levels in WT and *rib* SGs during cell invagination, we propose that *rib* regulates the production and/or activity of an unidentifed Moe phosphatase, a regulator of Prl-1 or Slik activity, or a Rho1 GAP, either directly or as part of an unidentified signaling cascade functioning subsequent to invagination.

Modulation of rib phenotype through Crb and Moe

We examined whether it was possible to rescue and mimic the *rib* phenotype through modulation of the levels and/or activity of Crb and Moe. High-level expression of full-length

Crb (Crb^{FL}) in the SG resulted in aberrant Crb localization and failed to rescue the *rib* defects, and low-level expression resulted in normal Crb localization but still failed to rescue the *rib* defects (data not shown). In addition, both high- and low-level expression of Crb^{FL} in the TR resulted in aberrant Crb localization and failed to rescue the *rib* defects (data not shown). Surprisingly, low-level expression of only the intracellular domain of Crb (Crb^{IC}), which contains the predicted Moe binding domain (Klebes and Knust, 2000), resulted in partial rescue of the *rib* DT defects (from 98.1% to 74.8% defective, p=3.0e-8; Figs. 4F, G) but failed to rescue the SG defects significantly (Fig. 4C, p=0.407). Similarly, expression of dominant negative Moe^{T559A} resulted in partial rescue of the *rib* DT defects (partial migration increased from 12.6% to 31.5%, for all defects p=0.00035; Figs. 4F, H) but still failed to rescue the SG defects (Fig. 4D).

We next sought to mimic the *rib* phenotype. *crb* hypomorphic alleles resulted in apical-basal polarity defects, obscuring any effects on tube morphogenesis (data not shown). However, expression of constitutively active Moe^{T559D} in WT embryos mimicked the *rib* phenotype both in the SG (69.7% defective; p<1.0e-8; Fig. 3M) and DT (44.2% defective; p<1.0e-8; Fig. 3N). Expression of Moe^{WT} in WT embryos resulted in a similar but less penetrant SG phenotype (16.4% defective; p=0.002; Fig. 3M) and WT-comparable DT morphology (16.0% defective with bias towards moderate class; p=0.215; Fig. 3N), further supporting the dependence of this phenocopy on Moe activity. The basis for more effective rescue in the DT and more effective phenocopy in the SG remains unclear, but we propose that differences in tube morphogenesis between these two organs may contribute. From these results, we conclude that near-physiological levels of expression of Crb^{FL} in the SG and TR are insufficient to rescue the *rib* defects, and we propose that expression of Crb^{IC} may result in partial rescue due to a dominant negative effect on Moe or another Crb binding partner. Finally, we conclude that increased Moe activity is a major contributor to the *rib* mutant SG and TR phenotypes.

TEM analysis of rib SGs reveals apical morphological defects

Ultrastructural analysis of stage 12 SGs by TEM revealed relatively normal epithelial cell structure in *rib* mutants, with columnar cells, basally positioned nuclei, and intact adherens junctions (Fig. 5). At this stage, WT SGs have turned and migrated on the visceral mesoderm (VM), with elongated lumena and a cellular apical-basal axis perpendicular to the lumen (Fig. 5A). In contrast, both moderate (Fig. 5E) and severe (Fig. 5I) *rib* SGs exhibited short lumena with the apical-basal axis tilted towards the distal end of the tube. The cells at the distal tip of *rib* SGs were also longer than those of WT (brackets in Figs. 5A, E, I). At higher magnification (4800x), WT SGs exhibited abundant apical membrane in the form of irregular microvillus-like structures that lay along the apical cell surface, rarely protruding into the SG lumen and most clearly seen where the TEM section skimmed across the cell surface before entering the cytoplasm (Figs. 5B-D). Moderate (Figs. 5F-H) and severe (Figs. 5J-L) *rib* SGs also exhibited abundant apical membrane, but this membrane was organized into longer and thinner structures that more closely resembled true microvilli and frequently protruded into the SG lumen. Additionally, at high magnification (15000x), WT SGs possessed numerous round vesicles adjacent to the apical membrane (arrowheads in Figs. 5B'-D', S3). Interestingly, these vesicles were smaller and less numerous in moderate *rib* SGs (arrowheads in Figs. 5F'-H', S4) and were rarely observed in severe *rib* SGs (arrowheads in Figs. 5J'-L', S5). Thus, TEM analysis indicates that *rib* SGs have generally normal epithelial cell architecture but exhibit short lumena with distally tilted apical-basal cell axes. In addition, *rib* SGs exhibit decreased numbers of apical vesicles and increased microvillar structure.

rib SG and TR exhibited WT-comparable levels and localization of the general secretory vesicle marker Cysteine String Protein and of the general endocytic vesicle marker Avalanche (Buchner and Gundersen, 1997; Lu and Bilder, 2005), suggesting that *rib* mutants do not exhibit

defects in general vesicular trafficking (data not shown). However, the vesicular marker Rab11 localized to an extreme apical position, comparable to that of the observed vesicles (Figs. 6A, C), and exhibited greatly reduced staining in *rib* SG and TR (Figs. 6B, D), consistent with reduced numbers of these vesicles in *rib* mutants. Rab11 is a well-conserved GTPase with key roles in targeted membrane delivery and recycling during cell shape changes (Pelissier et al., 2003; Saraste and Goud, 2007; Satoh et al., 2005; Strickland and Burgess, 2004). In polarized epithelia, Rab11 localizes to apical recycling endosomes (Hoekstra et al., 2004) as well as to apically-targeted secretory vesicles emerging directly from the Golgi (Satoh et al., 2005), suggesting that the apical vesicle population observed by TEM may constitute a system for apical membrane delivery and/or rearrangement during SG tube elongation.

Discussion

Here, we have shown that loss of *lolal*, which encodes a BTB-domain containing protein identified as a Rib interacting protein by a genome-wide yeast two hybrid screen (Faucheux et al., 2003; Giot et al., 2003; Siegmund and Lehmann, 2002), leads to *rib*-like defects in the SG and DT that are enhanced by the additional removal of one functional copy of *rib*. Moreover, *lolal* is required for robust nuclear localization of Rib in all primary epithelia, an activity likely mediated through the BTB domains of both proteins, since a point mutation in the BTB domain of *rib* leads to a complete loss of its nuclear accumulation (Figs. 1P, S) and since Lolal contains very little sequence outside its BTB domain (Faucheux et al., 2003). We demonstrated that loss of *rib* and *lolal* result in diminished expression of *crb*, which encodes an apical membrane protein required for overall cell polarity and apical membrane expansion (Izaddoost et al., 2002; Johnson et al., 2002; Pelissier et al., 2003; Wodarz et al., 1995). Loss of *rib* also independently affected the phosphorylation state of Moe, a protein known for its role in cross-linking apical membrane proteins, such as Crb, to the underlying actin cytoskeleton (Medina et al., 2002; Polesello et al., 2002). We further demonstrated that the phosphorylation state of Moe is a key factor in Rib-mediated tube elongation. Finally, our ultrastructural analysis revealed two defects in *rib* mutant salivary glands, both of which localize to the apical domain of the cells and both of which are consistent with known roles of Crb and Moe.

A model for Rib and Lolal function

We propose the following model. During epithelial tube morphogenesis, Rib and Lolal function to directly or indirectly upregulate transcription of *crb* and an *unknown factor* (*uf*) downregulating apical Moe activity (phosphorylation). In WT epithelia, increased Crb levels and decreased apical Moe activity lead to increased numbers of apical vesicles, decreased linkage of apical membrane and cytoskeleton, and decreased microvillar structure during tube elongation (Fig. 7A). Conversely, in *rib* epithelia, failure to upregulate transcription of *crb* and *uf* result in fewer apical vesicles, robust membrane-cytoskeleton linkage and increased microvillar structure during tube elongation (Fig. 7B).

Crb is required for the establishment and maintenance of apical-basal polarity and for expansion of apical membrane during tissue differentiation (Laprise et al., 2006; Omori and Malicki, 2006; Pellikka et al., 2002; Tepass and Knust, 1993). Moreover, forced *crb* overexpression expands the apical plasma membrane domain in several embryonic tissues, including the SG (Myat and Andrew, 2002; Wodarz et al., 1995). Recent studies have shown that epithelial polarity in early embryos is actively maintained by exocyst-dependent apical localization of Crb (Blankenship et al., 2007). The exocyst complex and another complex that includes the small GTPase Rab11 have been implicated in the delivery of vesicles from both recycling endosomes and the Golgi to the plasma membrane, playing key roles in apical membrane expansion during photoreceptor cell differentiation (Beronja et al., 2005; Langevin et al., 2005; Li et al., 2007; Satoh et al., 2005). Rab11 binds Sec5, a protein in the exocyst

complex, suggesting that the two complexes work together to facilitate apical vesicular transport (Beronja et al., 2005). In early embryos, mutations in the Exo84 subunit of the exocyst complex also disrupt the normal apical punctate staining of Rab11, although somewhat later than the disruption in Crb localization is observed, suggesting that Rab11-mediated apical trafficking may be Crb dependent (Blankenship et al., 2007). Correlating with the reduced levels of Crb observed in *rib* and *lolal* mutants (Fig. 2), our TEM and confocal analyses revealed a significant loss of Rab11-coincident apical vesicles in *rib* mutant salivary glands (Figs. 5, 6). We propose that these apically-localized Rab11 vesicles are Crb-dependent structures that provide a source of membrane that contributes to apical membrane expansion during tube elongation. Our finding that expression of wild-type Crb fails to rescue tube elongation in *rib* mutants, however, suggests that reduced Crb expression is not the limiting factor in Rib-mediated tube elongation.

rib SG and TR cells also exhibit high apical levels of pMoe (Fig. 3), a known cross-linker of F-actin and membrane-associated proteins (Medina et al., 2002;Polesello et al., 2002). Our TEM analysis indicates that *rib* cells have increased microvillar structure (Fig. 5), a phenotype consistent with increased linkage of membrane and cytoskeleton and in agreement with ERM family function in Drosophila photoreceptors and murine enterocytes (Karagiosis and Ready, 2004;Saotome et al., 2004). Furthermore, we demonstrated that expression of constitutively active Moe in SG and TR mimics the *rib* phenotype (Fig. 3). The corresponding activating mutation in the Moe homolog Ezrin has been shown to dramatically increase actin binding times in vertebrate cell microvilli (Coscoy et al., 2002). Consistent with this finding, increased activity of the ERM-related protein Band 4.1 has been shown to correlate with increased membrane stiffness in vertebrate erythrocytes (Manno et al., 2005). Moreover, a recent study has shown that expression of constitutively active Moe (the same phosphomimetic used in this study) increases cortical rigidity in Drosophila S2 cells, whereas loss of Moe or overexpression of dominant-negative Moe has the opposite effect (Kunda et al., 2008). Thus, the elevated apical Moe activity observed in *rib* mutant SG and TR should increase cortical rigidity of the apical region and increase resistance to its deformation. Although diminished levels of Crb and Rab11-coincident apical vesicles may also serve to increase resistance to deformation by limiting apical membrane growth and/or rearrangement, our genetic studies suggest that changes in the activity state of Moe may be the limiting step in tube elongation.

BTB proteins and transcriptional control of morphogenesis

BTB domain transcription factors (BTB-TFs) have been implicated in tumorigenesis, developmental regulation of homeotic genes, and modification of higher-order chromatin structure (Kelly and Daniel, 2006; Lehmann, 2004; Siegmund and Lehmann, 2002). In Drosophila, most BTB-TFs possess either Pipsqueak (PS) or Zinc Finger (ZF) DNA-binding domains (Siegmund and Lehmann, 2002). Drosophila BTB-TFs appear to interact with each other via the BTB domain independent of the type of DNA-binding domain (Faucheux et al., 2003; Ferres-Marco et al., 2006; Schwendemann and Lehmann, 2002). From such studies, a picture is emerging wherein BTB-TFs function in a combinatorial fashion with GAGA Factor, the Polycomb and Trithorax families, or other chromatin remodeling complexes to activate or repress gene transcription (Lehmann, 2004). Indeed, Lolal is required for enhanced Rib nuclear localization in only primary epithelia, indicating that Rib partners with other proteins, potentially other BTB-TFs, for its robust nuclear localization and function in mesodermal tissues. The same yeast two-hybrid studies that identified Lolal as a Rib interacting protein also identified Diskette, which encodes Drosophila Ada3, a subunit of the GCN5 histone acetyltransferase complex that has recently been shown to be required for histone modification and gene-specific transcriptional activation (Grau et al., 2008). Thus, transcriptional activation of *crb* and other Rib targets may be mediated through interactions between Rib and the GCN5 complex.

The extensive interaction seen among Drosophila PS and ZF BTB-TFs may be of relevance to vertebrates, as the PS group appears unique to Drosophila while the ZF group has expanded in vertebrates to around eighty members (Perez-Torrado et al., 2006). This suggests the exciting possibility that a morphogenic cassette orthologous to Rib and Lolal may exist among vertebrate BTB-TFs with ZF domains. Since Crb and Moe are well conserved in vertebrates, we propose that similar morphogenic cassettes may operate in vertebrate tissue development and remodeling, perhaps regulated by zinc finger BTB domain orthologues of Rib and Lolal (Perez-Torrado et al., 2006). Indeed, an exciting future no doubt awaits as investigators continue to uncover the transcriptional control of tube elongation during tissue development and disease.

Lumenal growth in both the SG and TR is regulated by other cellular events at later stages, specifically the secretion and subsequent modifications of an apical matrix (Abrams et al., 2006; Tsarouhas et al., 2007). In the WT trachea, immediately following the fusion of DT into a contiguous tube, there is an apical exocytic burst that drives uniform diametrical swelling of the lumen (Tsarouhas et al., 2007). The secreted materials include chitin as well as several unknown proteins that form a transient chitinous matrix that coordinates uniform radial expansion of the DT tubes (Araujo et al., 2005; Devine et al., 2005; Moussian et al., 2006; Tonning et al., 2006; Tonning et al., 2005). Subsequent modification of the chitinous matrix by chitin deacetylases, encoded by the *serpentine* (*serp*) and *vermiform* (*verm*) genes, is required to limit tube elongation (Luschnig et al., 2006; Wang et al., 2006). Interestingly, high level expression of *serp* and *verm* requires *rib* (Luschnig et al., 2006), indicating that Rib may regulate expression of different classes of genes to coordinate stage-specific aspects of lumenal expansion. Here, we show that at early stages Rib is required in both the SG and TR to regulate *crb* expression and Moe activity to allow for lumenal elongation. At late stages, Rib appears to be required for high-level TR expression of *verm* and *serp* to limit TR tube elongation (Luschnig et al., 2006). Although a requirement for a secreted apical matrix in the maintenance of uniform open SG lumena has also been demonstrated (Abrams et al., 2006; Seshaiah et al., 2001), Rib function has not yet been linked to expression of any of the proteins required for the formation of this matrix.

In summary, we propose that the decreased levels of *crb* and increased levels of active Moe observed in *rib* mutants increase resistance to apical deformation, providing a mechanistic basis for the incomplete lumenal elongation observed in *rib* mutant SG and DT. In related work, we test if this increased rigidity in only a thin apical domain can account for the failure in tube elongation in *rib* mutants (Cheshire et al., submitted).

Supplementary Material

Refer to Web version on PubMed Central for supplementary material.

ACKNOWLEDGEMENTS

We would like to thank members of the Andrew lab, Ann Hubbard and Carolyn Machamer for helpful discussions; Carol Cooke for assistance with TEM; David Bilder, Pamela Bradley, Douglas Cavener, Richard Fehon, Shigeo Hayashi, Mark Krasnow, Hiroki Oda, Donald Ready, Christos Samakovlis, Laurent Theodore, Bloomington, DSHB, and Flybase for fly stocks and reagents; Allan Spradling and Michael Buszczak for embryo sorting equipment and assistance; Pere Puigserver for RT-PCR equipment; Douglas Barrick, Pamela Bradley, Ann Hubbard, Carolyn Machamer and two anonymous reviewers for critical comments on the manuscript. This work was funded by a Whitaker Foundation Graduate Fellowship to A.M.C., NIH NIDCR Grants R01 DE12873 and R01 DE13899 to D.J.A.

REFERENCES

Abrams EW, Mihoulides WK, Andrew DJ. Fork head and Sage maintain a uniform and patent salivary gland lumen through regulation of two downstream target genes, PH4alphaSG1 and PH4alphaSG2. Development 2006;133:3517–27. [PubMed: 16914497]

Araujo SJ, Aslam H, Tear G, Casanova J. mummy/cystic encodes an enzyme required for chitin and glycan synthesis, involved in trachea, embryonic cuticle and CNS development-Analysis of its role in Drosophila tracheal morphogenesis. Dev Biol 2005;288:179–93. [PubMed: 16277981]

Beronja S, Laprise P, Papoulas O, Pellikka M, Sisson J, Tepass U. Essential function of Drosophila Sec6 in apical exocytosis of epithelial photoreceptor cells. J Cell Biol 2005;169:635–46. [PubMed: 15897260]

Blankenship JT, Fuller MT, Zallen JA. The Drosophila homolog of the Exo84 exocyst subunit promotes apical epithelial identity. J Cell Sci 2007;120:3099–110. [PubMed: 17698923]

Bradley PL, Andrew DJ. ribbon encodes a novel BTB/POZ protein required for directed cell migration in Drosophila melanogaster. Development 2001;128:3001–15. [PubMed: 11532922]

Bradley PL, Myat MM, Comeaux CA, Andrew DJ. Posterior migration of the salivary gland requires an intact visceral mesoderm and integrin function. Dev Biol 2003;257:249–62. [PubMed: 12729556]

Brand AH, Perrimon N. Targeted gene expression as a means of altering cell fates and generating dominant phenotypes. Development 1993;118:401–415. [PubMed: 8223268]

Buchner E, Gundersen C. The DnaJ-like cysteine string protein and exocytotic neurotransmitter release. Trends Neurosci 1997;20:223–227. [PubMed: 9141199]

Coscoy S, Waharte F, Gautreau A, Martin M, Louvard D, Mangeat P, Arpin M, Amblard F. Molecular analysis of microscopic ezrin dynamics by two-photon FRAP. Proc Natl Acad Sci U S A 2002;99:12813–12818. [PubMed: 12271120]

Devine WP, Lubarsky B, Shaw K, Luschnig S, Messina L, Krasnow MA. Requirement for chitin biosynthesis in epithelial tube morphogenesis. Proc Natl Acad Sci U S A 2005;102:17014–9. [PubMed: 16287975]

Faucheux M, Roignant JY, Netter S, Charollais J, Antoniewski C, Theodore L. batman interacts with polycomb and trithorax group genes and encodes a BTB/POZ protein that is included in a complex containing GAGA factor. Mol Cell Biol 2003;23:1181–95. [PubMed: 12556479]

Ferres-Marco D, Gutierrez-Garcia I, Vallejo DM, Bolivar J, Gutierrez-Avino FJ, Dominguez M. Epigenetic silencers and Notch collaborate to promote malignant tumours by *Rb* silencing. Nature 2006;439:430–6. [PubMed: 16437107]

Fievet B, Louvard D, Arpin M. ERM proteins in epithelial cell organization and functions. Biochim Biophys Acta 2007;1773:653–660. [PubMed: 16904765]

Forte E, Orsatti L, Talamo F, Barbato G, De Francesco R, Tomei L. Ezrin is a specific and direct target of protein tyrosine phosphatase PRL-3. Biochim Biophys Acta 2008;1783:334–44. [PubMed: 18078820]

Giot L, Bader JS, Brouwer C, Chaudhuri A, Kuang B, Li Y, Hao YL, Ooi CE, Godwin B, Vitols E, Vijayadamodar G, Pochart P, Machineni H, Welsh M, Kong Y, Zerhusen B, Malcolm R, Varrone Z, Collis A, Minto M, Burgess S, McDaniel L, Stimpson E, Spriggs F, Williams J, Neurath K, Ioime N, Agee M, Voss E, Furtak K, Renzulli R, Aanensen N, Carrolla S, Bickelhaupt E, Lazovatsky Y, DaSilva A, Zhong J, Stanyon CA, Finley RL Jr. White KP, Braverman M, Jarvie T, Gold S, Leach M, Knight J, Shimkets RA, McKenna MP, Chant J, Rothberg JM. A protein interaction map of *Drosophila melanogaster*. Science 2003;302:1727–36. [PubMed: 14605208]

Grau B, Popescu C, Torroja L, Ortuno-Sahagun D, Boros I, Ferrus A. Transcriptional adaptor ADA3 of Drosophila melanogaster is required for histone modification, position effect variegation, and transcription. Mol Cell Biol 2008;28:376–85. [PubMed: 17967867]

Henderson KD, Andrew DJ. Regulation and function of Scr, exd, and hth in the Drosophila salivary gland. Dev Biol 2000;217:362–74. [PubMed: 10625560]

Hipfner DR, Keller N, Cohen SM. Slik Sterile-20 kinase regulates Moesin activity to promote epithelial integrity during tissue growth. Genes Dev 2004;18:2243–8. [PubMed: 15371338]

Hoekstra D, Tyteca D, van ISC. The subapical compartment: a traffic center in membrane polarity development. J Cell Sci 2004;117:2183–92. [PubMed: 15126620]

Hughes SC, Fehon RG. Understanding ERM proteins - the awesome power of genetics finally brought to bear. Curr Opin Cell Biol 2007;19:51–56. [PubMed: 17175152]

Isaac DD, Andrew DJ. Tubulogenesis in Drosophila: a requirement for the trachealess gene product. Genes Dev 1996;10:103–17. [PubMed: 8557189]

Izaddoost S, Nam SC, Bhat MA, Bellen HJ, Choi KW. Drosophila Crumbs is a positional cue in photoreceptor adherens junctions and rhabdomeres. Nature 2002;416:178–183. [PubMed: 11850624]

Jack J, Myette G. The genes raw and ribbon are required for proper shape of tubular epithelial tissues in Drosophila. Genetics 1997;147:243–53. [PubMed: 9286684]

Johnson K, Grawe F, Grzeschik N, Knust E. Drosophila crumbs is required to inhibit light-induced photoreceptor degeneration. Curr Biol 2002;12:1675–80. [PubMed: 12361571]

Karagiosis SA, Ready DF. Moesin contributes an essential structural role in Drosophila photoreceptor morphogenesis. Development 2004;131:725–732. [PubMed: 14724125]

Kelly KF, Daniel JM. POZ for effect - POZ-ZF transcription factors in cancer and development. Trends Cell Biol 2006;16:578–87. [PubMed: 16996269]

Kerman BE, Cheshire AM, Andrew DJ. From fate to function: the Drosophila trachea and salivary gland as models for tubulogenesis. Differentiation 2006;74:326–48. [PubMed: 16916373]

Klämbt C, Glazer L, Shilo B-Z. *breathless*, a Drosophila FGF receptor homolog, is essential for migration of tracheal and specific midline glial cells. Genes & Dev 1992;6:1668–1678. [PubMed: 1325393]

Klebes A, Knust E. A conserved motif in Crumbs is required for E-cadherin localisation and zonula adherens formation in Drosophila. Curr Biol 2000;10:76–85. [PubMed: 10662667]

Kunda P, Pelling AE, Liu T, Baum B. Moesin controls cortical rigidity, cell rounding, and spindle morphogenesis during mitosis. Curr Biol 2008;18:91–101. [PubMed: 18207738]

Langevin J, Morgan MJ, Sibarita JB, Aresta S, Murthy M, Schwarz T, Camonis J, Bellaiche Y. Drosophila exocyst components Sec5, Sec6, and Sec15 regulate DE-Cadherin trafficking from recycling endosomes to the plasma membrane. Dev Cell 2005;9:355–76.

Laprise P, Beronja S, Silva-Gagliardi NF, Pellikka M, Jensen AM, McGlade CJ, Tepass U. The FERM protein Yurt is a negative regulatory component of the Crumbs complex that controls epithelial polarity and apical membrane size. Dev Cell 2006;11:363–74. [PubMed: 16950127]

Lehmann M. Anything else but GAGA: a nonhistone protein complex reshapes chromatin structure. Trends Genet 2004;20:15–22. [PubMed: 14698615]

Lehmann, R.; Tautz, D. *In situ* Hybridization to RNA.. In: Goldstein, LSB.; Fyrberg, EA., editors. *Drosophila melanogaster*: Practical Uses in Cell and Molecular Biology. 44. Academic Press; San Diego: 1994. p. 755

Li BL, Satoh AK, Ready DF. Myosin V, Rab11, and dRip11 direct apical secretion and cellular morphogenesis in developing Drosophila photoreceptors. Journal of Cell Biology 2007;177:659–669. [PubMed: 17517962]

Lu H, Bilder D. Endocytic control of epithelial polarity and proliferation in Drosophil. Nat Cell Biol 2005;7:1232–1239. [PubMed: 16258546]

Luschnig S, Batz T, Armbruster K, Krasnow MA. serpentine and vermiform encode matrix proteins with chitin binding and deacetylation domains that limit tracheal tube length in Drosophila. Curr Biol 2006;16:186–94. [PubMed: 16431371]

Manning, G.; Krasnow, M. Development of the Drosophila tracheal system.. In: Bate, M.; Martinez Arias, M., editors. The Development of Drosophila melanogaster. I. Cold Spring Harbor Laboratory Press; Cold Spring Harbor: 1993. p. 609-686.

Manno S, Takakuwa Y, Mohandas N. Modulation of erythrocyte membrane mechanical function by protein 4.1 phosphorylation. J Biol Chem 2005;280:7581–7. [PubMed: 15611095]

Medina E, Lemmers C, Lane-Guermonprez L, Le Bivic A. Role of the Crumbs complex in the regulation of junction formation in Drosophila and mammalian epithelial cells. Biol Cell 2002;94:305–13. [PubMed: 12500938]

Moussian B, Tang E, Tonning A, Helms S, Schwarz H, Nusslein-Volhard C, Uv AE. Drosophila Knickkopf and Retroactive are needed for epithelial tube growth and cuticle differentiation through their specific requirement for chitin filament organization. Development 2006;133:163–71. [PubMed: 16339194]

Myat MM, Andrew DJ. Fork head prevents apoptosis and promotes cell shape change during formation of the Drosophila salivary glands. Development 2000a;127:4217–26. [PubMed: 10976053]

Myat MM, Andrew DJ. Organ shape in the Drosophila salivary gland is controlled by regulated, sequential internalization of the primordia. Development 2000b;127:679–91. [PubMed: 10648227]

Myat MM, Andrew DJ. Epithelial tube morphology is determined by the polarized growth and delivery of apical membrane. Cell 2002;111:879–91. [PubMed: 12526813]

Nishimura M, Inoue Y, Hayashi S. A wave of EGFR signaling determines cell alignment and intercalation in the Drosophila tracheal placode. Development 2007;134:4273–82. [PubMed: 17978004]

Omori Y, Malicki J. oko meduzy and related crumbs genes are determinants of apical cell features in the vertebrate embryo. Curr Biol 2006;16:945–57. [PubMed: 16713951]

Pelissier A, Chauvin JP, Lecuit T. Trafficking through Rab11 endosomes is required for cellularization during Drosophila embryogenesis. Curr Biol 2003;13:1848–1857. [PubMed: 14588240]

Pellikka M, Tanentzapf G, Pinto M, Smith C, McGlade CJ, Ready DF, Tepass U. Crumbs, the Drosophila homologue of human CRB1/RP12, is essential for photoreceptor morphogenesis. Nature 2002;416:143–149. [PubMed: 11850625]

Perez-Torrado R, Daisuke Y, Defossez PA. Born to bind: the BTB protein-protein interaction domain. BioEssays 2006;28:1194–1202. [PubMed: 17120193]

Pfaffl MW. A new mathematical model for relative quantification in real-time RTPCR. Nucleic Acids Res 2001;29:e45. [PubMed: 11328886]

Polesello C, Delon I, Valenti P, Ferrer P, Payre F. Dmoesin controls actin-based cell shape and polarity during *Drosophila melanogaster* oogenesis. Nat Cell Biol 2002;4:782–789. [PubMed: 12360288]

Preacher, KJ. Calculation for the chi-square test: An interactive calculation tool for chi-square tests of goodness of fit and independence. 2001.

Reuter R, Panganiban GEF, Hoffmann FM, Scott MP. Homeotic genes regulate the spatial expression of putative growth factors in the visceral mesoderm of *Drosophila* embryos. Development 1990;110:1031–1040. [PubMed: 1983113]

Saotome I, Curto M, McClatchey AI. Ezrin is essential for epithelial organization and villus morphogenesis in the developing intestine. Dev Cell 2004;6:855–64. [PubMed: 15177033]

Saraste J, Goud B. Functional symmetry of endomembranes. Mol Biol Cell 2007;18:1430–1436. [PubMed: 17267686]

Satoh AK, O'Tousa JE, Ozaki K, Ready DF. Rab11 mediates post-Golgi trafficking of rhodopsin to the photosensitive apical membrane of Drosophila photoreceptors. Development 2005;132:1487–1497. [PubMed: 15728675]

Schwendemann A, Lehmann M. Pipsqueak and GAGA factor act in concert as partners at homeotic and many other loci. Proc Natl Acad Sci U S A 2002;99:12883–8. [PubMed: 12271134]

Seshaiah P, Miller B, Myat MM, Andrew DJ. pasilla, the Drosophila homologue of the human Nova-1 and Nova-2 proteins, is required for normal secretion in the salivary gland. Dev Biol 2001;239:309–22. [PubMed: 11784037]

Shiga Y, Tanaka-Matakatsu M, Hayashi S. A nuclear GFP/β-galactosidase fusion protein as a marker for morphogenesis in living Drosophila. Develop. Growth Differ 1996;38:99–106.

Shim K, Blake KJ, Jack J, Krasnow MA. The Drosophila ribbon gene encodes a nuclear BTB domain protein that promotes epithelial migration and morphogenesis. Development 2001;128:4923–33. [PubMed: 11731471]

Siegmund T, Lehmann M. The Drosophila Pipsqueak protein defines a new family of helix-turn-helix DNA-binding proteins. Dev Genes Evol 2002;212:152–7. [PubMed: 11976954]

Speck O, Hughes SC, Noren NK, Kulikauskas RM, Fehon RG. Moesin functions antagonistically to the Rho pathway to maintain epithelial integrity. Nature 2003;421:83–7. [PubMed: 12511959]

Strickland LI, Burgess DR. Pathways for membrane trafficking during cytokinesis. Trends Cell Biol 2004;14:115–118. [PubMed: 15055200]

Tepass U, Knust E. Crumbs and stardust act in a genetic pathway that controls the organization of epithelia in Drosophila melanogaster. Dev Biol 1993;159:311–26. [PubMed: 8365569]

Tonning A, Helms S, Schwarz H, Uv AE, Moussian B. Hormonal regulation of mummy is needed for apical extracellular matrix formation and epithelial morphogenesis in Drosophila. Development 2006;133:331–41. [PubMed: 16368930]

Tonning A, Hemphala J, Tang E, Nannmark U, Samakovlis C, Uv A. A transient luminal chitinous matrix is required to model epithelial tube diameter in the Drosophila trachea. Dev Cell 2005;9:423–30. [PubMed: 16139230]

Tsarouhas V, Senti KA, Jayaram SA, Tiklova K, Hemphala J, Adler J, Samakovlis C. Sequential pulses of apical epithelial secretion and endocytosis drive airway maturation in Drosophila. Dev Cell 2007;13:214–25. [PubMed: 17681133]

Vining MS, Bradley PL, Comeaux CA, Andrew DJ. Organ positioning in Drosophila requires complex tissue-tissue interactions. Dev Biol 2005;287:19–34. [PubMed: 16171793]

Wang S, Jayaram SA, Hemphala J, Senti KA, Tsarouhas V, Jin H, Samakovlis C. Septate-junction-dependent luminal deposition of chitin deacetylases restricts tube elongation in the Drosophila trachea. Curr Biol 2006;16:180–5. [PubMed: 16431370]

Weigel D, Bellen HJ, Jürgens G, Jäckle H. Primordium specific requirement of the homeotic gene *fork head* in the developing gut of the *Drosophila* embryo. Roux's Archiv Developmental Biology 1989;198:201–210.

Wilk R, Weizman I, Shilo BZ. trachealess encodes a bHLH-PAS protein that is an inducer of tracheal cell fates in Drosophila. Genes Dev 1996;10:93–102. [PubMed: 8557198]

Wodarz A, Hinz U, Engelbert M, Knust E. Expression of Crumbs confers apical character on plasma membrane domains of ectodermal epithelia of Drosophila. Cell 1995;82:67–76. [PubMed: 7606787]

Zelzer E, Shilo BZ. Interaction between the bHLH-PAS protein Trachealess and the POU-domain protein Drifter, specifies tracheal cell fates. Mech Dev 2000;91:163–73. [PubMed: 10704841]

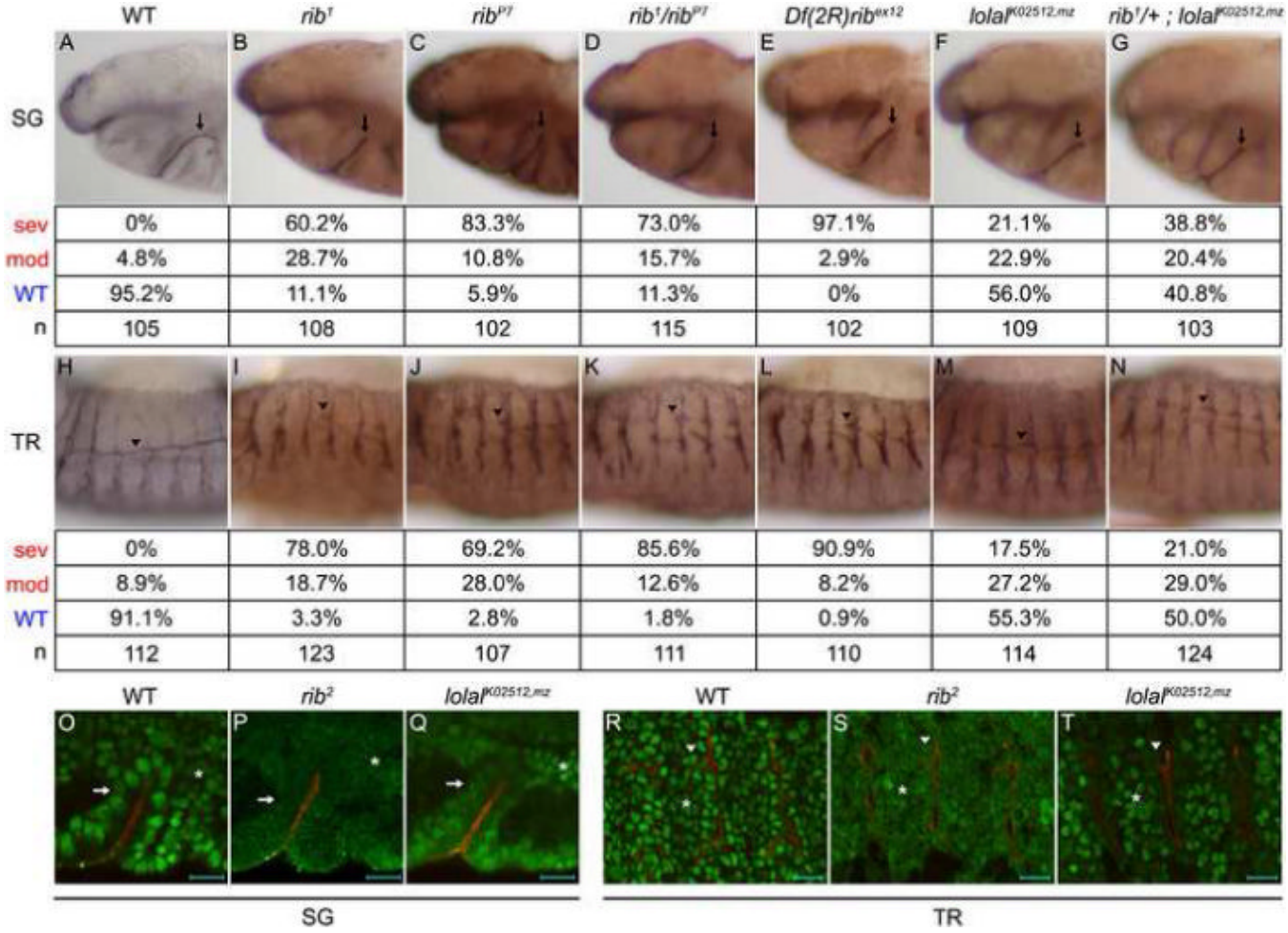

Fig. 1.

Lolal serves as a novel partner for Rib in SG and TR morphogenesis. (A-G) SG defects are observed in *rib* and *lolal*^{K02512,mz} mutants. Arrows indicate stage 12 SGs in WT (A), *rib* alleles (B-E), *lolal*^{K02512,mz} (F) and *rib*^{1}/+; *lolal*^{K02512,mz} (G) mutants. SG phenotypes were divided into three classes: WT (migrated, A), moderate (turned posteriorly but failed to migrate, F), and severe (failed to turn, B-E, G). (H-N) TR defects are observed in *rib* and *lolal*^{K02512,mz} mutants. Arrowheads indicate stage 14 DT of metamere 4 in WT (H), *rib* alleles (I-L), *lolal*^{K02512,mz} (M) and *rib*^{1}/+; *lolal*^{K02512,mz} (N) mutants. DT phenotypes were divided into three classes based on the distance migrated towards metamere 3: WT (greater than two-thirds, H), moderate (between one-and two-thirds, M, N), and severe (less than one-third, I-L). (O-T) An antibody to Rib shows loss of nuclear localization in *rib*^{2} mutants and of epithelial nuclear localization in *lolal*^{K02512,mz} mutants. Rib (green) exhibited robust nuclear localization in WT SG (arrow in O), TR (arrowhead in R), and adjacent mesoderm (asterisk in O,R) and failed to localize to the nuclei of all of these tissues in the *rib*^{2} BTB domain mutant (P,S). Rib exhibited weak nuclear localization in *lolal*^{K02512,mz} mutant SG (Q) and TR (T) but maintained robust nuclear localization in adjacent mesoderm. Embryos are stage 11 for SG and stage 12 for TR. Scale bars are 10 μm. An antibody to Sas marks SG and TR lumena in black (A, H), brown (B-G, I-N), or red (O-T). All embryos are oriented with dorsal up and anterior to the left unless otherwise noted.

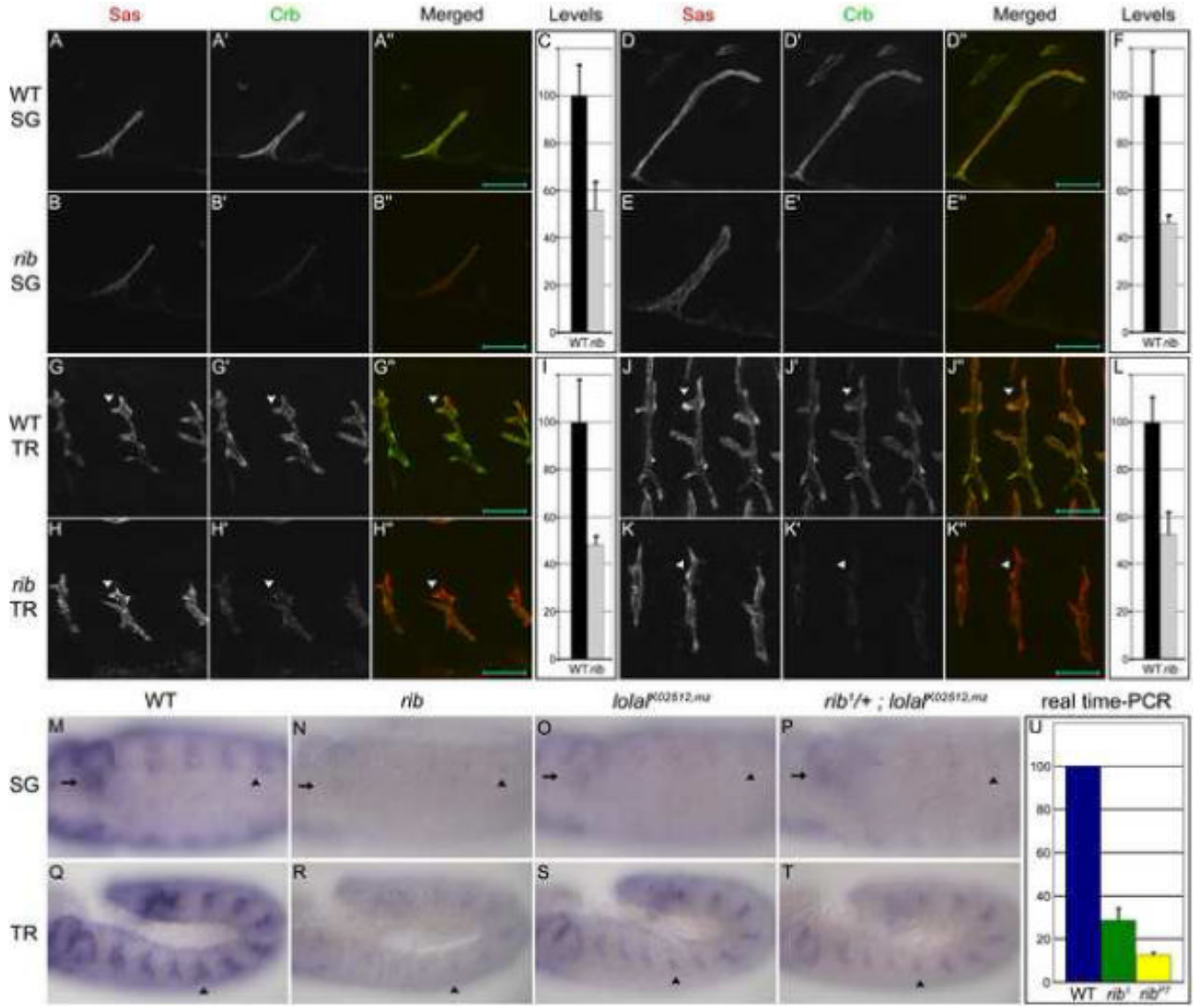

Fig. 2.

Rib and Lolal are required for robust *crb* expression. (A-L) *rib* mutants exhibited comparable Sas levels (red) but severely decreased Crb levels (green) during SG invagination (A, B) and migration (D, E) and TR primary branch formation (G, H) and elongation (J, K). Arrowheads in G, H, J, K indicate DT of metamere 4. Sas-normalized pixel intensity indicated that Crb levels were reduced by at least half in *rib* mutants (C, F, I, L). Images are maximum intensity projections of image stacks acquired under identical conditions. Crb/Sas ratios were averaged over three locations per organ in three embryos. Error bars show standard deviation of ratio. Scale bars are 20 μm. (M-U) *crb* expression is robust in WT SG (M) and TR (M, Q) but is severely reduced in *rib* (N, R), reduced in $lolal^{K02512,mz}$ (O, S), and slightly further reduced in rib^{1}/+; $lolal^{K02512,mz}$ (P, T) mutant embryos. M-P are ventral views and arrows mark SG. Arrowheads in M-T mark metamere 4. Quantitative real time-PCR on stage 12 embryos indicates that total *crb* mRNA levels are reduced by 71% in rib^{1} mutants and by 87% in rib^{P7} mutants (U). Error bars show standard deviation of three independent reactions.

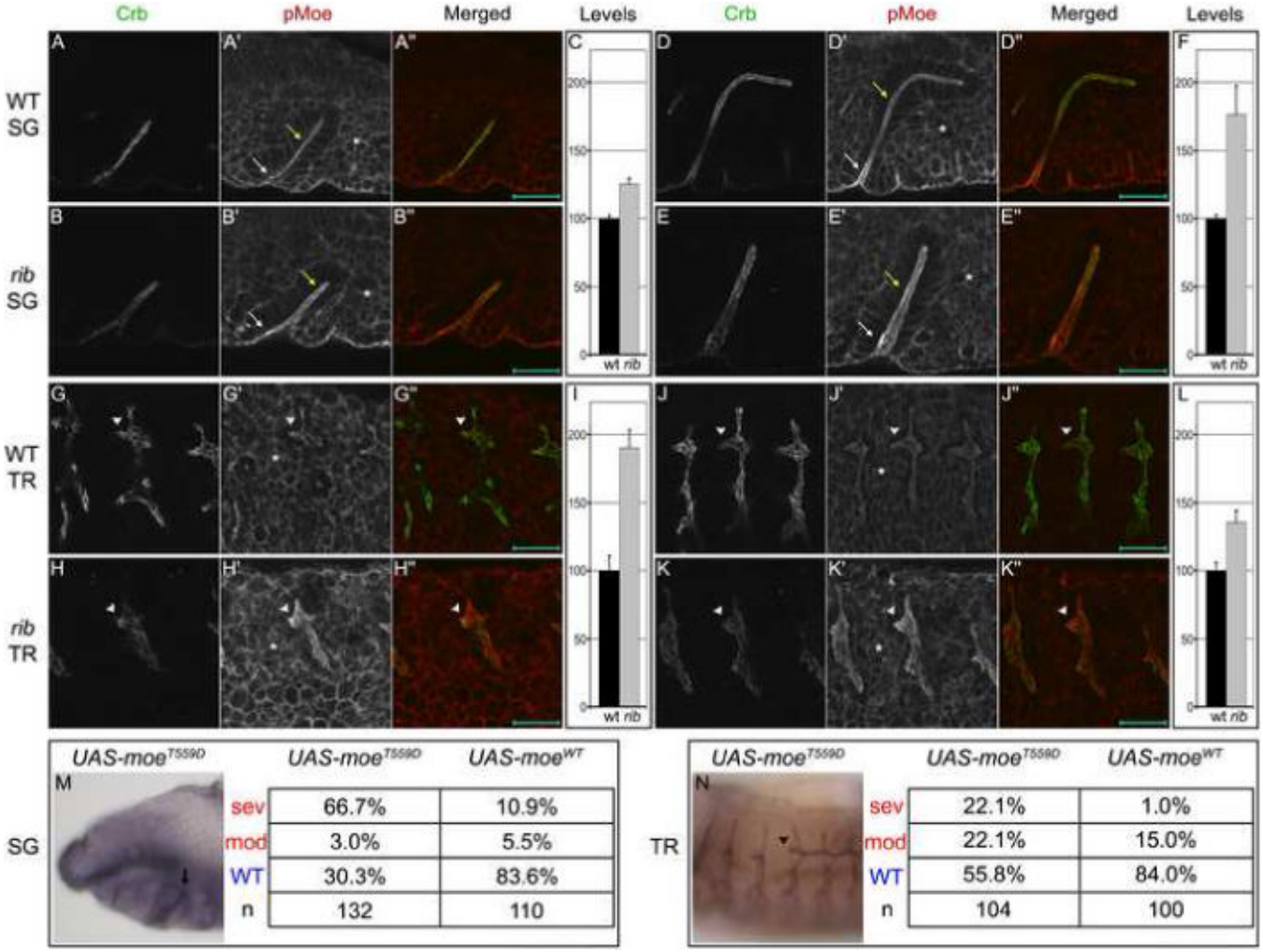

Fig. 3.

Rib is required for downregulation of apical Moe activity. (A-L) WT and *rib* SGs exhibited similarly high levels of apical pMoe (red) in invaginating cells (white arrows in A, B, D, E). After invagination, WT SG cells exhibited moderate, mesoderm-comparable (asterisk) levels (yellow arrows in A, D), whereas *rib* SG cells maintained the high invagination levels of pMoe (yellow arrows in B, E). WT TR exhibited moderate mesoderm-comparable levels of pMoe during primary branch formation and elongation (G, J), whereas *rib* TR exhibited relatively high levels of apical pMoe during these processes (H, K). Arrowhead in G, H, J, K indicates DT of metamere 4. Scale bars are 20 μm. Mesoderm-normalized apical pMoe pixel intensity indicated that *rib* SG and TR exhibit elevated levels of Moe activity (C, F, I, L). Images are single optical sections (to avoid photobleaching) acquired under identical conditions. Peak pMoe (apical)/ pMoe (mesoderm) ratios were averaged over three locations per organ in three embryos. Error bars show standard deviation of ratio. Crb is in green. (M-N) Tissue-specific expression of constitutively active Moe^{T559D} results in *rib*-like phenotypes in the stage 12 SG (arrow in M) and stage 14 DT (arrowhead in N). Phenotypes are categorized as in Fig. 1. An antibody to Sas marks the SG lumen in black (M) and DT lumen in brown (N).

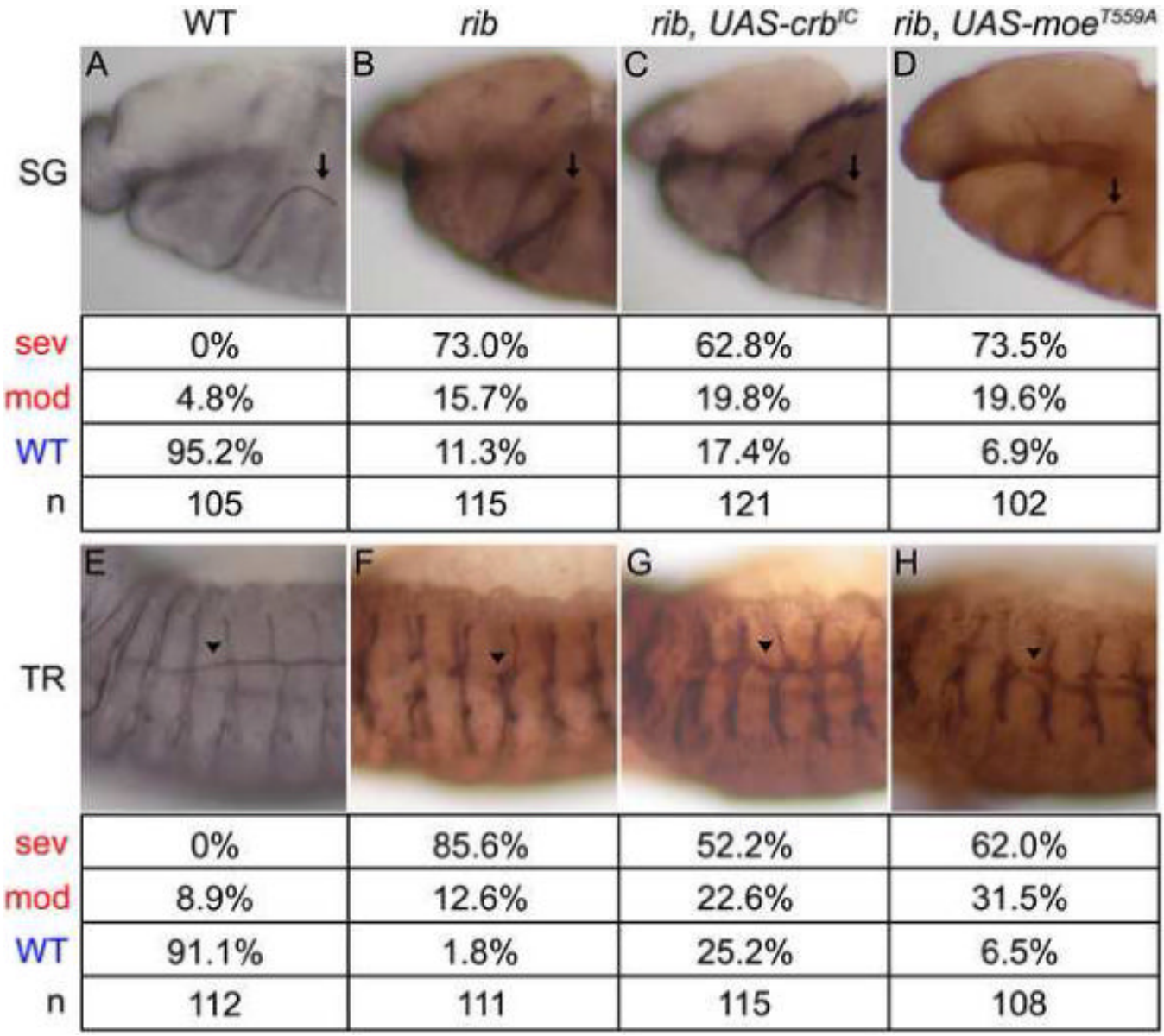

SG	WT	rib	rib, UAS-crb^{IC}	rib, UAS-moe^{T559A}
sev	0%	73.0%	62.8%	73.5%
mod	4.8%	15.7%	19.8%	19.6%
WT	95.2%	11.3%	17.4%	6.9%
n	105	115	121	102

TR	WT	rib	rib, UAS-crb^{IC}	rib, UAS-moe^{T559A}
sev	0%	85.6%	52.2%	62.0%
mod	8.9%	12.6%	22.6%	31.5%
WT	91.1%	1.8%	25.2%	6.5%
n	112	111	115	108

Fig. 4.

Intracellular domain of Crb and dominant negative Moe can partially rescue the *rib* DT defects. (A-D) Tissue-specific expression of the intracellular domain of Crb and dominant negative Moe fails to significantly rescue the *rib* SG defects. Expression is driven specifically in the SG using *fkh-Gal4*. Arrows indicate stage 12 SGs in WT (A), *rib* mutants (B), *rib* mutants with *fkh-Gal4* driving *UAS-Crb^{IC}* (C), and *rib* mutants with *fkh-Gal4* driving *UAS-Moe^{T559A}* (D). The salivary gland phenotypes are categorized as in Figure 1. (E-H) Tissue-specific expression of the intracellular domain of Crb and dominant negative Moe partially rescues the *rib* DT defects. Expression is driven specifically in the TR using *btl-Gal4*. Arrowheads indicate stage 14 DT of metamere 4 in WT (E), *rib* (F), *rib* with *btl-Gal4* driving *UAS-Crb^{IC}* (G), and *rib* with *btl-Gal4* driving *UAS-Moe^{T559A}* (H). The tracheal phenotypes are categorized as in Figure 1. An antibody to Sas marks the SG and TR lumena in black (A ,E) or brown (B-D, F-H). All embryos are oriented with dorsal up and anterior to the left.

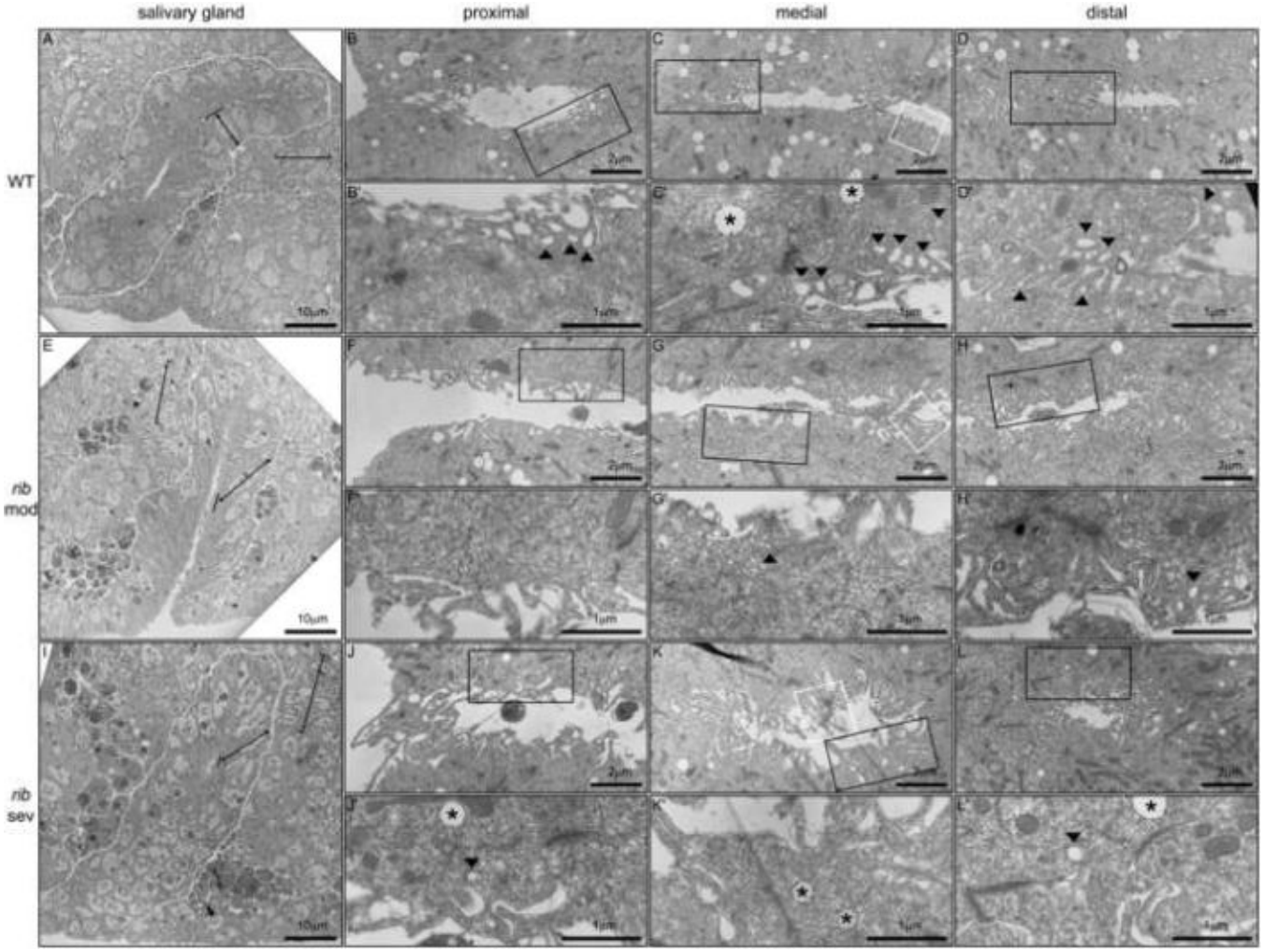

Fig. 5.

TEM of *rib* SGs reveals apical morphological defects. (A, E, I) WT and *rib* SGs shown at 980x magnification. Dotted line outlines stage 12 WT (A) and moderate (E) and severe (I) *rib* SGs. Apical-basal cell axis (double-headed arrow in A, E, I) is perpendicular to lumenal axis (line) in WT SGs (A) but tilted distally in *rib* SGs (E, I). Brackets indicate distal tip cells. (B-D, F-H, J-L) In *rib* mutants, increased microvillar structure is observed at proximal (compare B to F, J), medial (compare C to G, K), and distal locations (compare D to H, L) at 4800x magnification. Representative images are shown from thin sections acquired throughout the SG lumen, and white boxes outline examples of microvillar structure in WT and *rib* cells. (B'-D', F'-H', J'-L') 15000x magnification reveals reduced number and size of apical vesicles in *rib* mutants. Views correspond to areas outlined with black boxes. Black arrowheads indicate apical vesicles. Asterisks indicate fixation artifacts observed in all tissues of all samples in both genotypes. Full images of 15000x magnification are shown in Figs. S3-5.

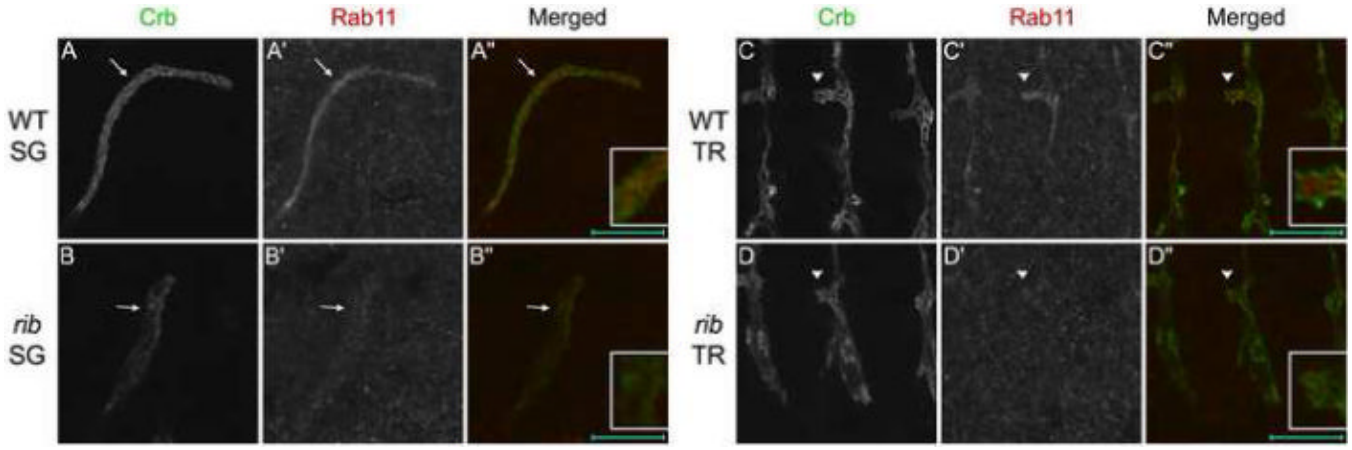

Fig. 6.

Decreased apical levels of the GTPase Rab11 suggest decreased membrane delivery and/or rearrangement in *rib* mutants. (A-D) Apical levels of the GTPase Rab11 (red) are severely decreased in *rib* mutants. WT SG (A) and TR (C) exhibit robust apical levels of the GTPase Rab11 during tube morphogenesis. During these same stages, *rib* SG (B) and TR (D) exhibit greatly reduced Rab11 levels, correlating with the relative depletion of subapical vesicles observed by TEM of *rib* mutant SG. See insets for higher magnification images of a portion of SG (arrows in A, B) and DT metamere 4 (arrowheads in C, D). Scale bars are 20 μm.

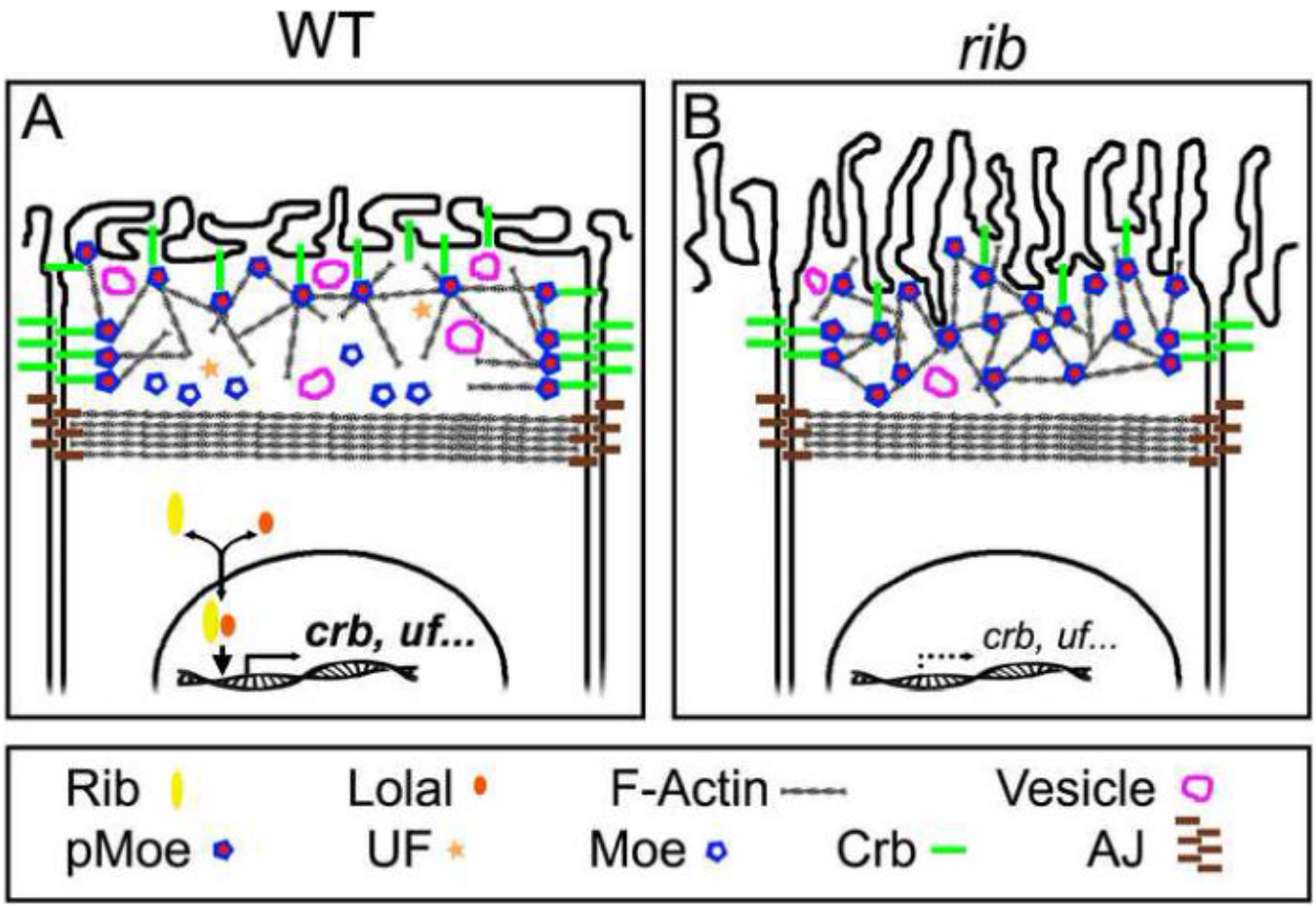

Fig. 7.

A cellular model for *rib* effects on apical membrane extension is shown. Ribbon and Lolal function to upregulate transcription of *crb* and an *unknown factor* (*uf*) required for Moesin dephosphorylation. (A) In wild-type cells, increased *crb* results in an increased population of apically-targetted Rab11 vesicles that fuse with the apical plasma membrane to allow for membrane growth. Decreased levels of active phosphorylated Moesin would result in less cross linking between the plasma membrane and the underlying actin cytoskeleton, and reduced microvilli, resulting in a less stiff apical surface. (B) In *ribbon* mutant cells, decreased *crb* results in fewer apically-targetted Rab11 vesicles to fuse with the apical plasma membrane, limiting its growth. Increased levels of active phosphorylated Moesin would result in more cross linking between the plasma membrane and underlying actin cytoskeleton and increased microvillar structure, resulting in a stiffer apical surface.

Table 1

The references/sources of fly lines used in this study.

Fly Line	Reference / Source
Oregon R	WT control
rib^{1}	Bloomington Stock Center
rib^{2}	Bloomington Stock Center
$lolal^{l(2)k02515}$	Bloomington Stock Center
rib^{P7}	Shim et al., 2001
Df(2R)rib^{ex12}	Shim et al., 2001
$lolal^{l(2)k02515}$; da-Gal4, UAS-lolalGFP / TM3,Sb	Faucheux et al., 2003
UAS-crb^{FL}	Wodarz et al., 1995
UAS-crb^{IC}	Wodarz et al., 1995
UAS-moe^{T559D}-myc	Karagiosis and Ready, 2004
UAS-moe^{T559A}	Speck et al., 2003
btl-Gal4	Shiga et al., 1996
fkh-Gal4	Henderson and Andrew, 2000

Table 2

Antibodies and antibody dilutions used in this study.

Antibody	Produced in	Dilution*	Reference / Source
Actin	Mouse	1:2000	MP Biomedicals, Inc.
Avl	Chicken	1:500	Lu and Bilder 2005
Crb	Mouse	1:10	DSHB†
Csp	Mouse	1:40	DSHB‡
GFP	Mouse	1:200	Molecular Probes
GFP	Rabbit	1:40000 / 1:10000	Molecular Probes
pMoe	Rabbit	1:500	Karagiosis and Ready, 2004
Rab11	Rabbit	1:500	Satoh et al., 2005
Rib	Rat	1:50	P. Bradley and D. Andrew, unpublished
SAS	Rabbit	1:5000 / 1:500	E. Organ and D. Cavener, unpublished
β-gal	Mouse	1:10000 / 1:500	Promega

*When appropriate, dilutions used both for HRP and fluorescence stainings are provided, respectively. Otherwise, only the dilution used for fluorescence staining is provided.

†The monoclonal antibody CQ4 developed by Elisabeth Knust was obtained from the Developmental Studies Hybridoma Bank (DSHB) developed under the auspices of the NICHD and maintained by The University of Iowa, Department of Biological Sciences, Iowa City, IA 52242.

‡The monoclonal antibody 6D6 developed by Seymour Benzer was also obtained from DSHB. Appropriate secondary antibodies conjugated to biotin (Vector Labs), Alexa Fluor 488, 555, 568, 647, or Rhodamine (Molecular Probes) were used in 1:500 dilution.